J Solid State Electrochem (1999) 3: 417–423

ORIGINAL PAPER

Keunjoo Kim · Hong Seub Kim · Hwack Joo Lee

Point-defect associated thermionic hole emissions from p-type Si/$Si_{1-x}Ge_x$/Si quantum well structures

Received: 22 August 1998 / Accepted: 15 February 1999

Abstract The thermionic hole emissions from a p-type $Si_{0.67}Ge_{0.33}$ quantum well with a width of 7 nm and a point defect were investigated using deep level transient spectroscopy. An activation energy of 0.22 eV from the quantum well is consistent with the heavy hole level from the bottom of the well. The defect-related band with an energy of 0.30 eV originated from the space charge related to the point defect in the vicinity of the quantum well heterostructure. The origin of the point-defect-related band was confirmed by photoluminescence and the deep level was further clarified by using capacitance-voltage measurements and simulation by introducing a simple model of an interfacial hole trap center. The deep hole trap center apparently disappeared by an annealing effect, indicating that point defects are subject to thermal annealing. The microscopic measurement provides evidence on point defects in the quantum well structure and the thermal annealing also enhances the thermionic hole emission from the quantum well structure.

Key words SiGe quantum well · Hole emission · Point defect · Molecular beam epitaxy growth · Deep level transient spectroscopy

Introduction

The band edge discontinuity in the heterostructures of semiconductor materials is an essential parameter determining device performance in band gap engineering. Most of the energy difference of band gaps in the Si/$Si_{1-x}Ge_x$/Si quantum well (QW) structures appears as a valence-band offset, which can be useful for quantum well infrared photodetectors (QWIP) [1–6] based on hole excitation across the QW barrier. The band offset is often determined by means of various optical and electrical measurements [7–10]. Photoluminescence (PL) is widely used to study electronic states in QWs [9]. The capacitance-voltage (C-V) measurement also provides useful information on carrier concentrations within the space-charge region of heterojunctions [7, 8]. Deep-level transient spectroscopy (DLTS) is a useful dynamic technique for the investigation of carrier capture and emission [7, 10]. DLTS usually can be utilized to detect defects in bulk states. When the technique is used to study heterostructures, the data analysis needs careful interpretation of the signals from the well or a trap.

The thermionic hole emission from the QW formed by the valence band offset has been analyzed under the assumption of a negligible number of trap centers at the interface so that no perturbation by the thermal emission of carriers from the traps occurred [8, 11, 12]. Vescan et al. [9] showed that the DLTS signal from the single QW around 90 K is broadened due to the presence of SiGe islands of 5–10 nm height, and a relatively small and broad band around 230 K is similar to the sample without the QW structure in crystalline bulk Si. However, Wang et al. [13] suggested that the intensive peak of a minority carrier at 210 K is comparable to the signal from the QW at 100 K and is correlated with the formation of interfacial defects from the partial relaxation of misfit strains. Schmalz et al. [7] also reported that the extra band of the majority carrier with an activation energy of 0.42 eV is related to growth fault. In spite of these extensive studies, the origin of the measured DLTS signal as being due to the interface state is still uncertain and systematic investigation is required.

In this work, the band offset was determined by analyzing DLTS spectra originating from the ground state of the bound hole in the QW, and the hole trap center at

K. Kim (✉)
Department of Semiconductor Applications,
Ulsan College, 29 Mugeo 2nd Dong Ulsan 680-749, Korea

H.S. Kim
Anam Industrial Co., Buchon 421-160, Korea

H.J. Lee
Korea Research Institute of Standards and Science,
Taejon 305-600, Korea

the heterointerface also was investigated with thermal annealing treatment. The PL and C-V measurements provide evidence on the energy level of the hole trap state and trap density. By introducing a trap level, simulations also clarify the influence of the trap density on the concentration profile at various temperatures. The quality of the samples was evaluated by high-resolution transmission electron microscopy (HRTEM).

Experimental

The samples were prepared by solid-source molecular beam epitaxy (MBE) on p-type Si(100) substrates. The chemical cleaning processes used H_2SO_4 solution for organic materials and $HF{:}H_2O_2 = 1{:}4$ for the native oxide layer; to remove the remaining native oxide layer, a baking process at 900 °C for 5 min was carried out, prior to the growth of the homoepitaxial buffer layer of Si on a Si surface at 500 °C. The growth of QW structures was carried out at a substrate temperature of 500 °C in order to obtain the abrupt interface by suppressing the formation of interfacial SiGe islands. The $Si_{0.67}Ge_{0.33}$ QW layer with a width of 7 nm was sandwiched between a Si buffer layer (1 μm) on the substrate and a Si cap layer (0.4 μm). The QW width is smaller than the critical thickness of pseudomorphic growth of SiGe on Si predicted by Kim and Lee [14]. All these layers were uniformly doped with boron to a hole concentration of 3–5 $\times$ 10^{16} cm^{-3} in order to obtain the p-type QW structure. The annealing treatment was carried out at a temperature of 800 °C for 5 min in a N_2 atmosphere.

For the C-V and the DLTS measurements, junctions were formed by depositing Schottky diodes on the Si caps by evaporating 1-mm diameter Al dots without alloying. Ohmic contacts were fabricated on the back side of the wafers by evaporating the Al film followed by alloying at 480 °C in a N_2 atmosphere. The C-V measurements were used to determine the distribution of the carrier concentrations and the corresponding temperature-dependent behavior. A computer-aided DLTS was also used to measure the carrier emission from both the QW and defect centers. The low-temperature PL spectra were observed in backscattering geometry using 514.5 nm line excitation from an Ar^+ ion laser with a power of 100 mW at a temperature of 7 K. The morphology of the samples was investigated by an HRTEM (H9000-NAR) at 300 kV with a point resolution of 1.8 Å.

Results and discussion

Figure 1 shows the DLTS spectra of an as-grown QW structure for various filling voltages (V_f) with a rate window of 1000/s. During the measurements, a reverse bias was applied with a fixed value of −2.5 V, which was large enough to deplete the QW region at low temperature. Two signals of thermionic hole emissions were observed in two different temperature regions. Under the filling voltage of −2.0 V, the reduced rate window causes the DLTS signal to peak at the lower temperature, as shown in the inset of Fig. 1. For the DLTS signals from the QW emissions, the band offset at the heterointerface can be derived from the emission rate e_p of holes in a QW across the barrier region [15]:

$$e_p = \frac{m^*_{Si}}{m^*_{SiGe}} \frac{kT}{h} \exp\left(-\frac{E_a}{kT}\right) \quad (1)$$

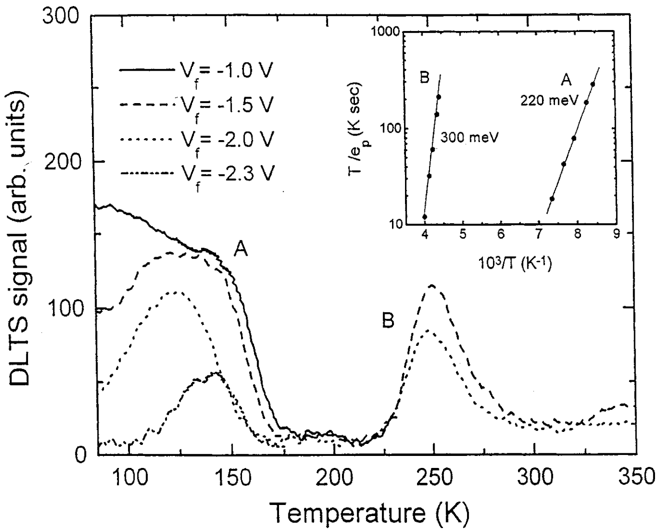

Fig. 1 DLTS spectra on the as-grown sample of the single $Si/Si_{0.67}Ge_{0.33}/Si$ quantum well structure. The two bands *A* and *B* are related to the hole emission from the quantum well and the deep-level defect center, respectively. The *inset* shows the activation energies from *A* (0.22 eV) and *B* (0.30 eV) bands under the filling voltage of −2.0 V. As the rate window for the data is decreased to 1000, 400, 200, 80, and 50/s, the temperature of the peak position is lowered correspondingly

where m^*_{Si} and m^*_{SiGe} are the effective hole masses of Si and SiGe for a given Ge composition of $x = 0.33$, respectively; h is the Planck constant, k is the Boltzmann constant, and E_a is the activation energy, which is the difference in energy between the first hole subband E_1 and the top of the well at the valence band edge. The valence-band offset ΔE_v can be given by the following relation:

$$\Delta E_v = E_1 + E_a + e\Delta V \quad (2)$$

where ΔV is the potential difference between the two sides of the well, and e is the charge of the electron.

The activation energies for thermionic hole emissions from a quantum state and a defect state to the valence band were obtained from the Arrhenius plot with values of 220 and 300 meV for bands A and B, respectively. According to People and Bean [16] and Tagaki et al. [17], the valence band offset value is estimated to be $\Delta E_v = 240$ meV for the $Si_{0.67}Ge_{0.33}/Si$ single QW structure and the highest level of the hole states is 18 meV below the bottom of the QW for the hole. This quantum state of the holes is comparable with the activation energy of band A to thermally excite holes in the QW. Note that a small band lowering caused by thermally assisted tunneling across the barrier at the junction boundary is attributed to an electric field effect [8, 13].

Band A was broadened with decreasing filling voltage and showed a shift of the DLTS peaks. The band broadening effect was correlated with interfacial states and with the presence of misfit dislocations [15, 18, 19]. Chretien et al. [20] have observed a broad signal in the high-temperature grown samples and they suggested that it was caused by the thickness variation of the SiGe layer due to island formation near the heterointerfaces. Although the higher growth temperature leads to a better quality of crystal, the high-temperature growth results in a rough and smeared interface and a dopant segregation. Therefore, in practice, epitaxial growth is usually carried out at a temperature range of 450–600 °C. However, this leads to introducing a high density of interfacial states and so the generation of band B.

Band B is activated with an energy of 0.3 eV, which indicates correlation with the hole state of deep levels. Several authors [7, 18, 19, 21] provide activation energies of deep levels for various Ge compositions, as shown in Fig. 2. The activation energy decreased with increasing Ge mole fraction. This implies that the deep level hole emission originates from the defect states correlated with the QW structure. The decrease of the band gap energy in pseudomorphic $Si_{1-x}Ge_x/Si$ heterostructures is proportional to the Ge mole composition and mainly influences the increase of the valence band offset, providing the enhanced electrical mobility and the reduced optical band gap in the Si layer [17, 22]. The activation energy for the point-defect-associated hole emission is also correlated with the valence band offset of the intrinsic band gap of SiGe as follows:

$$E_a(x) = E_a(0) - 0.75x \text{ (eV)} \tag{3}$$

where $E_a(0)$ is the activation energy in the Si deep level and x is the Ge composition. This indicates that the point defect resides in the QW or in the vicinity of the heterointerface.

The origin of band B was further clarified by a thermal annealing effect, which can reduce defect states in both interface and bulk structures. The samples were annealed at 800 °C for 5 min in a nitrogen atmosphere and the DLTS results are shown in Fig. 3. Only one peak was observed at the same temperature as band A and an activation energy of 230 meV was obtained, which is similar to the as-grown sample, indicating thermionic hole emission from the QW structure. Furthermore, the broad and small DLTS signals became very intensive and band B apparently disappeared. This

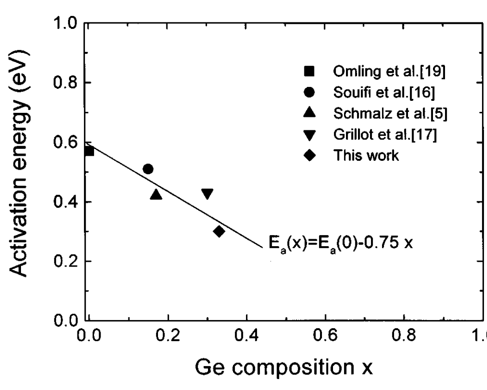

Fig. 2 The activation energy of defect-related hole emission in terms of the Ge mole composition. The valence band offset influences the activation energy for the deep level hole emission

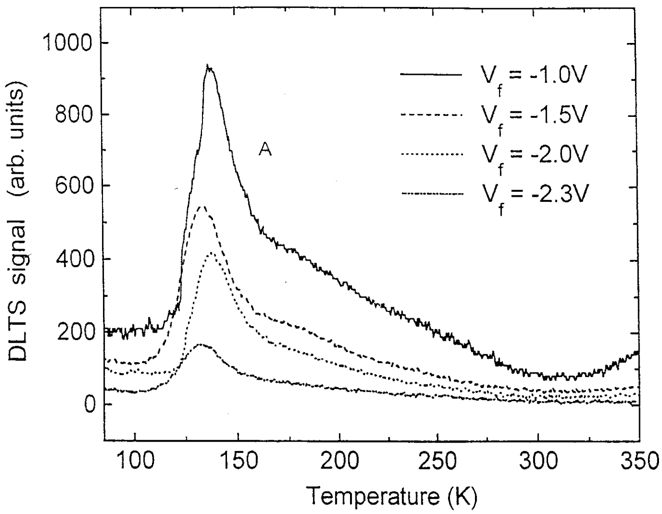

Fig. 3 DLTS spectra on the annealed sample at a temperature of 800 °C for 5 min. Band *B* is dramatically annealed out and band *A* becomes more intense. The activation energy is slightly increased to a value of 0.23 eV, indicating a slight deformation of the shape of the quantum well structure

indicates that the deep level is related to space charges of the point defect which can be annealed out so that the corresponding hole emission from the hole trap center to the valence band ceases in the annealed sample. Furthermore, in QWIP devices, the photo-excited hole can be related to the enhanced quantum efficiency by the annealing effect. Further evidence of the origin of the deep state was provided by PL measurements.

Figure 4 shows the low-temperature PL spectra of the as-grown sample with the SiGe layer (a) and the corresponding sample annealed at 800 °C for 5 min (b). Both samples show the clear transverse optical phonon replica of the bound exciton (BE) of c-Si at 1.08 eV and the annealed sample shows the free exciton (FE) level just above the BE from the c-Si layer. The contribution of

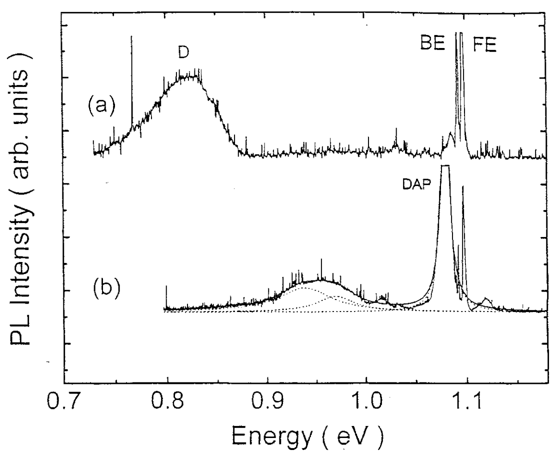

Fig. 4 PL spectra of an as-grown sample (*a*) containing a $Si_{0.67}Ge_{0.33}$ layer and the correspondingly annealed sample (*b*). The defect-related PL band at the peak energy of 0.82 eV with a large full width at half maximum of 60 meV disappeared under thermal annealing

defect-related electronic states to the PL band in SiGe/Si heterostructures has been reported [9, 23, 24]. The defect-related peak in PL spectra appears with no band-to-band peaks at a low deposition temperature of 600 °C. On increasing the deposition temperature, the defect-related peak disappears and the band-to-band peaks occur. The dislocation-related PL bands are located at 0.81 (D_1) and 0.87 eV (D_2) [24–26]. Our broad band around 0.70–0.85 eV peaked at 0.82 eV and is similar to the dislocation-related band of D_1 except for the broadness, and it disappeared in the thermally annealed sample. This disappearence indicates that the broad PL band does not originate from misfit dislocations, which can not disappear by annealing, but to point defects. However, the annealed sample shows a broad peak at 0.95 eV from a QW structure and a small peak at 1.02 eV which seems to correspond to the *TO*-Γ phonon replica of an electron-hole droplet in the Si substrate. Also a strong *TO* phonon replica of the droplet is observed at about 1.08 eV.

The point-defect-associated PL band may be related to the hole emission band of the DLTS peak B in Fig. 1, because the defect-related PL band peak with an energy of 0.82 eV is consistent with the localized hole state B above the valence band with an activation energy of 0.3 eV. The positive space charge around the heterointerfaces of the SiGe/Si structure plays an important role in a hole trap center where electrons excited by optical energy can recombine with the holes at the defect center. The defect center may influence the electrical behavior of the hole carrier in the QW structure, so a detailed C-V profile was studied.

Shown in Fig. 5 are the hole carrier spikes resulting from the valence-band offset of the strained SiGe/Si heterojunction. At room temperature, hole carriers are

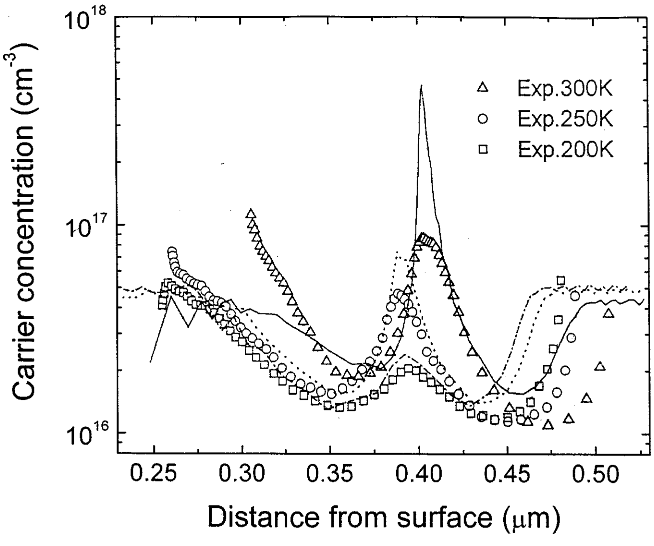

Fig. 5 Apparent carrier concentration profiles obtained from 1-MHz C-V measurements for the as-grown QW at various temperatures. The simulations (*solid/dashed lines*) were performed under the conditions of hole traps: $D^0_{it} = 3.5 \times 10^{11}$ cm^{-2} and $E_a = 0.1$ eV

confined in the partially depleted QW region. The concentration of the hole carrier decreases with decreasing temperature and the QW region is completely depleted below a temperature of 200 K. This anomalous behavior is correlated with the defect states owing to the low-temperature growth. In the normal situation, the quantum well should confine more carriers at the lower temperature [27]. It is valuable to note that the C-V profiles were normal for as-grown samples at temperatures higher than 650 °C and/or those at temperatures less than 500 °C with low Ge compositions. Since the defect states localized in the band gap strongly attract holes to be trapped in the center, it can be expected that hole states influence the C-V results. This can be quantitatively analyzed by simulation, including the hole capture mechanism.

To simulate the apparent profile of carriers, an enhanced version of the technique introduced by Missous and Rhoderick and others [27–29] was implemented to numerically solve Poisson's equation. The effect of gap states was taken into account with information about the quantized energy level in the QW structure. The electric field can be perturbed by defect states at the interface as follows:

$$\epsilon_{i+1} \left.\frac{d\phi}{dx}\right|_{i+1} = \epsilon_i \left.\frac{d\phi}{dx}\right|_i + qD_{it} \tag{4}$$

where ϵ, ϕ, q, and D_{it} are the dielectric constant, the electric potential, the electric charge, and the deep trap density, respectively. The temperature-dependent trap density of hole states is written as

$$D_{it}(T) = \frac{D^0_{it}}{1 + e^{(E_{pF} - E_t)/kT}} \tag{5}$$

where D^0_{it} represents the unactivated trap density of hole states at 0 K and E_{pF} and E_t ($= E_{pF} + E_a$) denote the hole quasi-Fermi level for the QW and the trap energy of the hole states from the Si valence band, respectively; E_a is the activation energy of the trap center from the quasi-Fermi level. For an unactivated hole density of $D^0_{it} = 3.5 \times 10^{11}$ cm^{-2} and an activation energy of $E_a = 0.1$ eV, the carrier concentration of the profile decreases as the temperature decreases and the QW region is fully depleted below a temperature of 200 K. This is in relatively good agreement with the experimental results.

The signal broadening in the DLTS measurement and the anomalous C-V characteristics in the as-grown QW structure are attributed to gap states originating from hole trap centers. The trap centers are positively charged with captured holes. The hole captured in the center needs an activation energy of 0.3 eV to be emitted. On the other hand, the quasi-Fermi level is located near the bottom of the QW with an estimated energy of $E_{pF} = 0.2$ eV above the valence band of Si for the boron doping level of 3–5 $\times 10^{16}$ cm^{-3}. The C-V simulation indicates that the deep level distributed above the quasi-Fermi level is located with an energy of $E_t = 0.3$ eV from the valence band edge. This is consistent with the

PL result for the defect-related band around 0.3 eV above the valence band.

The schematic energy diagram of the hole emission transient process under reverse bias is illustrated in Fig. 6. By applying the filling pulse with a reverse bias of -2.5 V in DLTS measurements, the holes occupy both the ground heavy hole state of the QW and the hole trap center in the vicinity of the QW. When the filling pulse completely disappears, the holes are emitted from both the QW and the defect state into the Si barrier, providing the bands A and B. Figure 7 shows that the simulated carrier profile is strongly dependent on the activation energy of the defect level. The carrier concentration is severely suppressed by increasing the activation energy. When the trap level is activated with an energy of $E_a = 0.2$ eV, the QW region is almost depleted for the trap density of $D_{it}^{0} = 3.5 \times 10^{11}$ cm^{-2}.

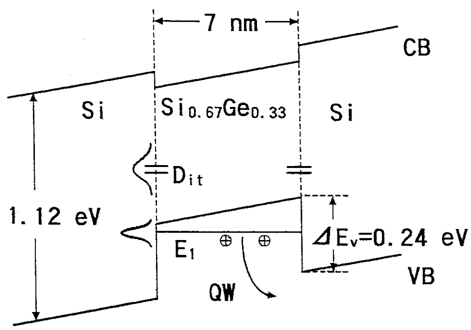

Fig. 6 Schematic band structure of the single quantum well formed by p-type $Si_{1-x}Ge_x$ with a Ge mole fraction of $x = 0.33$ under reverse bias. The defect-related PL center at 0.82 eV from the conduction band shows the hole trap level, which is activated with an energy of 0.3 eV. The QW-related heavy hole state provides the hole emission with an activation energy of 0.22 eV

The thermal annealing process is very effective at reducing the density of the gap states. Figure 8 shows normal C-V profiles for the annealed sample at 800 °C for 5 min. The peaks of the hole carriers are very sharp even at low temperature, indicating that the gap states are no longer the dominant source of hole capture in the annealed sample. The defect-free nature of the annealed sample is demonstrated by the simulation without any gap state, providing the normal aspect of the enhanced carrier concentration of the QW structure at a low temperature.

In order to understand the quality of the as-grown and the annealed samples of the $Si/Si_{0.67}Ge_{0.33}/Si$ epilayer, transmission electron microscopy (TEM) images were obtained. Figure 9 shows the cross-sectional bright field micrographs. The as-grown sample in Fig. 9a shows the inclusion of the dislocation line with the smeared QW layer. However, the annealed sample in Fig. 9b provides the defect-free structure with the well-defined line of the QW layer. Furthermore, the high resolution TEM images in Fig. 10 show the different structural quality of the crystalline phase in the vicinity of the QW layer. In the as-grown sample of Fig. 10a the randomly oriented contrasts (arrows) show as point defects distributed in the cap layer and the QW region rather than behaving as localized interfacial defects. The point-defect sites are positively charged and provide deep levels for radiative recombination centers in PL. These delocalized defect sites also provide hole emission centers in DLTS measurements.

Usually, in the lattice mismatched heterointerface, the misfit dislocations, once formed, are hard to remove by thermal annealing. In contrast, the thermal annealing may cause the release of the misfit strain, resulting in an increasing density of dislocations. The defect-free QW structure with well-defined heterointerfaces indicates

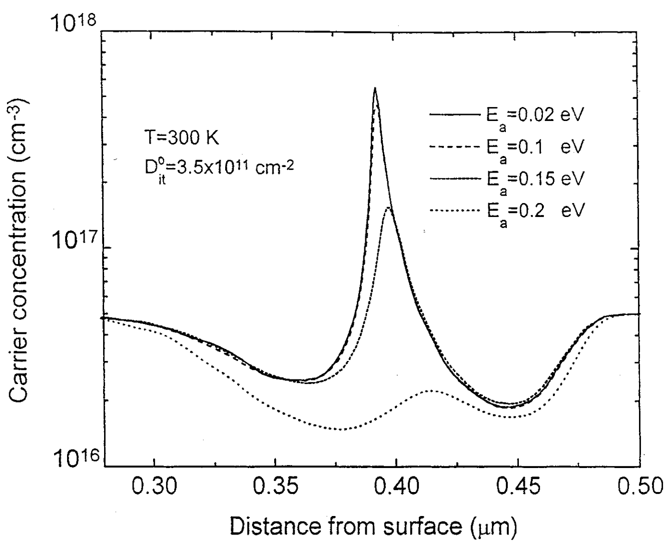

Fig. 7 Simulated carrier profiles from the QW structure for various activation energies at room temperature. The spike of the carrier concentration is strongly decreased with increasing the activation energy

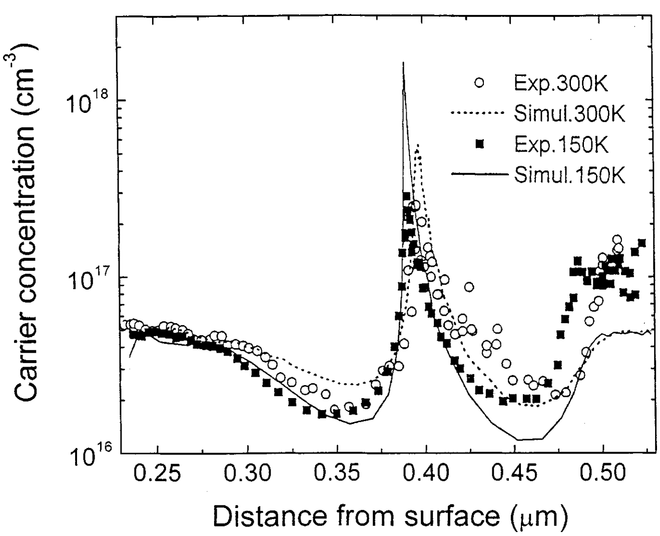

Fig. 8 Apparent carrier concentration profiles for the annealed sample at different temperatures. The concentration is increased with lowering the temperature without the carrier capture. The simulation was performed without the interfacial defect center

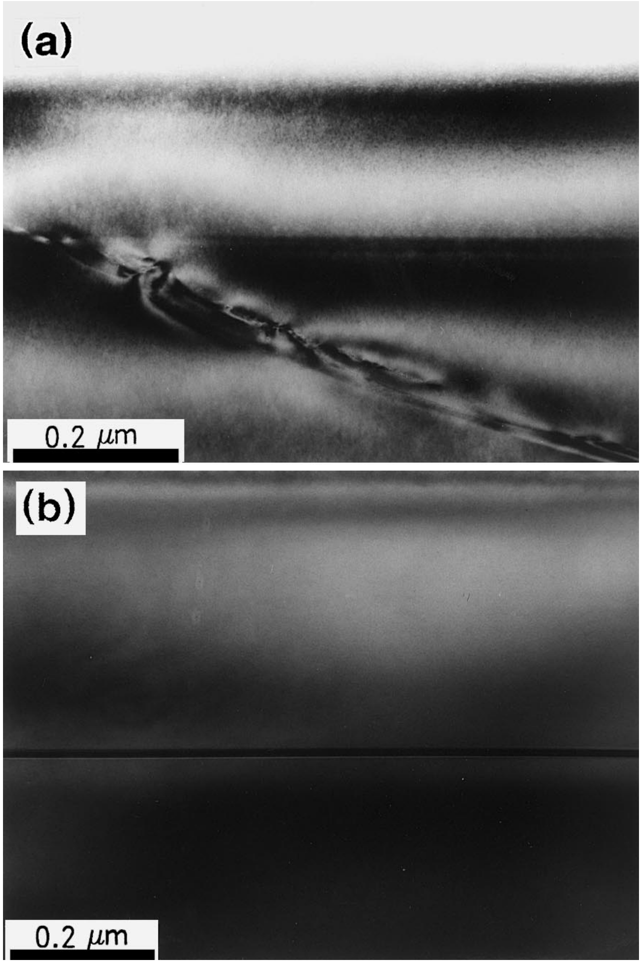

Fig. 9 The cross-sectional bright field TEM images on **a** the as-grown $Si/Si_{0.67}Ge_{0.33}/Si$ layer and **b** the corresponding thermally annealed sample at a temperature of 900 °C for 5 min. In the image of the as-grown sample, there exists a dislocation line with a smeared line of the QW layer. The annealed sample shows a clear straight-line image for the QW layer

that the defect-related peak B of the hole emission in Fig. 1 was annealed. The SiGe QW layer is subjected to a strain field between the Si buffer and the cap layers by showing diffraction contrast without any misfit dislocation. Note that for the SiGe heterointerfaces with a Ge composition of $x = 0.33$ the thermal annealing induces Ge diffusion in the SiGe alloy [30]. The reconstructed heterointerfaces by the annealing effect enhance thermionic hole emission from the quantized hole state of the valence band offset and the point defect-related hole emission is terminated.

Conclusions

In summary, the thermionic hole emission processes from both the QW and the defect structures were investigated by means of the DLTS measurement and C-V characteristics. The thermionic emission of holes bound

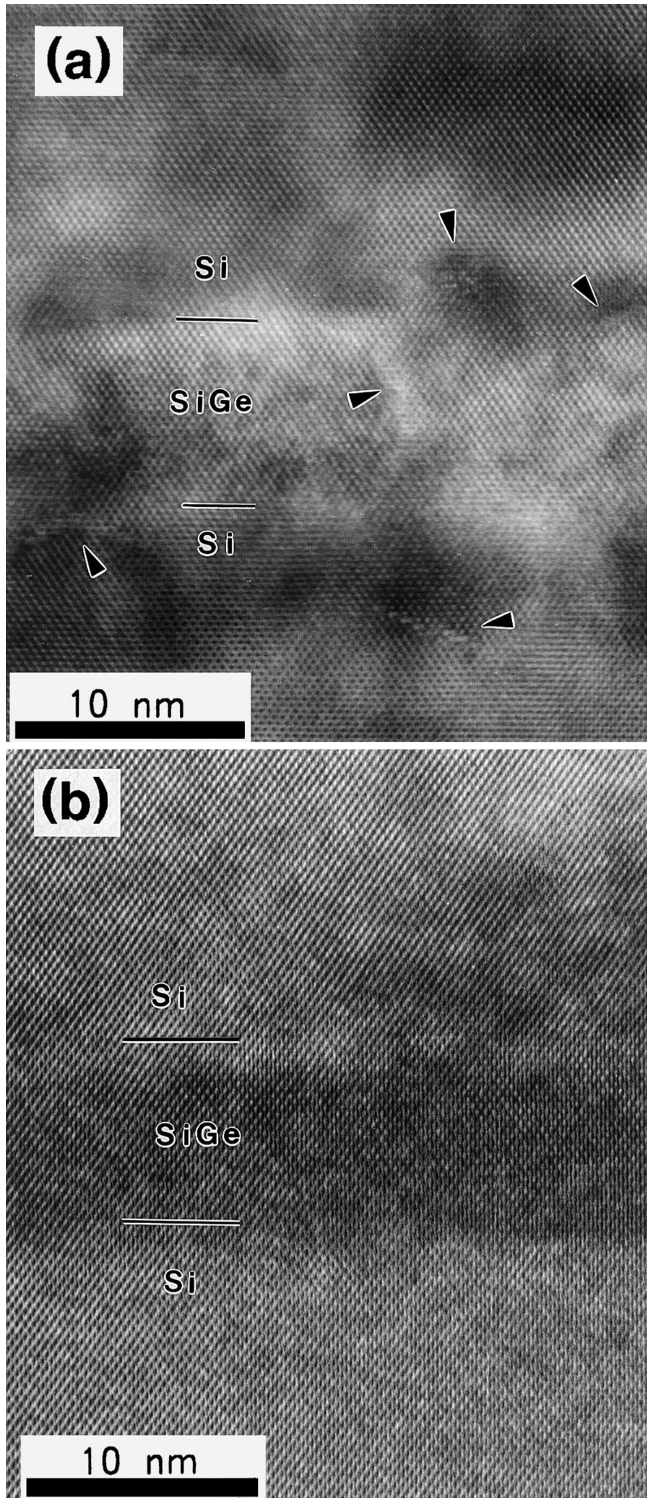

Fig. 10 HRTEM images on **a** the as-grown $Si/Si_{0.67}Ge_{0.33}/Si$ layer and **b** the corresponding thermally annealed sample at a temperature of 900 °C for 5 min. In the image of the as-grown sample there are many delocalized point defects (*arrows*) in the vicinity of the heterointerfaces. The point defects were annealed out and the misfit strain was released for the interfacial reconstruction

in the QW structure is activated with an energy of 0.22 eV. The hole emission is activated with an energy of 0.3 eV from the point defects randomly distributed in the cap layer and QW region. The annealing effect strongly reduces the concentration of the hole trap center of the point defects compared with that of the QW signal. The defect-related bands in both the DLTS and PL measurements disappeared after thermal annealing. Furthermore, in the C-V measurement, the anomalous decreasing trend of the carrier concentration on lowering the temperature is changed to an increase by the annealing effect. As a concluding remark, the relatively low temperature growth of the $Si_{1-x}Ge_x$ QW structure with a Ge mole fraction of $x = 0.33$ provides randomly distributed spots of point defects. The crystal point-defects-associated hole emission is perturbed by the misfit strain, which influences the distribution of the electronic structure in the vicinity of the QW structure.

References

1. People R (1986) IEEE J Quantum Electron 22: 1696
2. Tsaur BY, Chen CK, Marino SA (1991) IEEE Electron Dev Lett 12: 293
3. Xiao X, Sturm JC, Parihar SR, Lyon SA, Meyerhofer D, Falfrey S, Shalleross FV (1993) IEEE Electron Dev Lett 14: 199
4. Whall TE, Parker EHC (1995) J Mater Sci Mater Electron 6: 249
5. Carline RT, Robbins DJ, Stanaway MB, Leong WY (1996) Appl Phys Lett 68: 544
6. Chang YC, James RB (1989) Phys Rev B 39: 12672
7. Schmalz K, Yassievich IN, Rücker H, Grimmeiss HG, Frankenfeld H, Mehr W, Osten HJ, Schley P, Zeindl HP (1994) Phys Rev B 50: 14287
8. Nauka K, Kamins TI, Turner JE, King CA, Hoyt JL, Gibbons JF (1992) Appl Phys Lett 60: 195
9. Vescan L, Hartmann A, Schmidt K, Dieker C, Lüth H (1992) Appl Phys Lett 60: 2183
10. Lang DV, People R, Bean JC, Sergent AM (1985) Appl Phys Lett 60: 197
11. Letartre X, Stievenard D, Lannoo M, Lippens D (1990) J Appl Phys 68: 116
12. Cavicchi RE, Lang DV, Gershoni D, Sergent AM, Vandenberg JM, Chu SNG, Panish MB (1989) Appl Phys Lett 54: 739
13. Wang Q, Lu F, Gong D, Chen X, Wang J, Sun H, Wang X (1994) Phys Rev B 50: 18226
14. Kim K, Lee YH (1995) Appl Phys Lett 67: 2212
15. Vescan L, Apetz R, Lüth H (1993) J Appl Phys 73: 7427
16. People R, Bean JC (1986) Appl Phys Lett 48: 538
17. Tagaki S, Hoyt JL, Rim K, Welser JJ, Gibbons JF (1998) IEEE Trans Electron Dev 45: 494
18. Souifi A, Bremond G, Benyattou T, Dutartre D, Berbezier I (1992) J Vac Sci Technol B 10: 2002
19. Grillot PN, Ringel SA, Fittgerald EA, Waston GP, Xie YH (1995) J Appl Phys 77: 676
20. Chretien O, Apetz R, Vescan L, Souifi A, Lüth H, Schmalz K, Koulmann JJ (1995) J Appl Phys 78: 5439
21. Omling P, Weber ER, Montelius L, Alexander H, Michel J (1985) Phys Rev B 32: 6571
22. Kim K, Suh MS, Shim HW, Youn CJ, Suh E-K, Lee KB, Lee HJ, Lee H-J, Ryu H (1997) Appl Phys Lett 71: 3007
23. Sauer R, Weber J, Stolz J (1983) Appl Phys A 36: 1
24. Tang HP, Vescan L, Dieker C, Schmidt K, Lüth H (1992) J Cryst Growth 125: 301
25. Vescan L, Dieker C, Hartmann A, Van der Hart A (1994) Semicond Sci Technol 9: 387
26. Chretien O, Apetz R, Vescan L (1996) Semicond Sci Technol 11: 1838
27. Tittelbach-Helmrich K (1993) Semicond Sci Technol 8: 1372
28. Missous M, Rhoderick EH (1985) Solid State Electron 28: 1372
29. Letartre X, Stievenard D, Barbier E (1991) Appl Phys Lett 58: 1047
30. Kim K, Kim HS, Kim JY, Lee YH, Lee HJ, Lee H-J, Ryu H (1997) J Solid State Electrochem 1: 221